An Experimental Analysis of an Impedance Pump as a
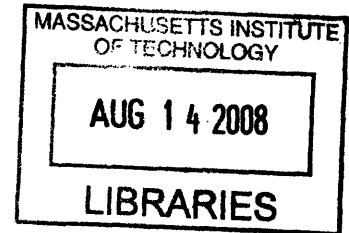# Model for Segmentation in the Intestine

by

Doria M. Holbrook

SUBMITTED TO THE DEPARTMENT OF MECHANICAL ENGINEERING IN
PARTIAL FULFILLMENT OF THE REQUIRMENT FOR THE DEGREE OF

BACHELOR OF SCIENCE IN MECHANICAL ENGINEERING
AT THE
MASSACHUSETTS INSTITUTE OF TECHNOLOGY

JUNE 2008

Signature of Author:_

Department of Mechanical Engineering
May 9, 2008

Certified by:_____

Anette Hosoi
Associate Professor of Mechanical Engineering
Thesis Supervisor

Accepted by:_

John H. Lienhard V
Professor of Mechanical Engineering
Chairman, Undergraduate Thesis Committee

An Experimental Analysis of an Impedance Pump as a
Model for Segmentation in the Intestine

by

Doria M. Holbrook

ABSTRACT

The intestine is a fluid-filled compliant tube that twists, turns, and folds back on itself, potentially causing changes in impedance of the tube. By asymmetrically compressing a compliant tube of physiological geometries with impedance changes, a net pressure head was induced. With Reynolds numbers ranging from 13-1350, the viscous and inertial effects of the fluid response created interesting pressure responses. The system was found to have a natural frequency near 1.69 Hz and exhibited frequency doubling. The dimensionless pressure and time responses showed a complicated pressure response that decreased in overall magnitude with increasing compression frequencies. The response is influenced by more parameters than just the compression frequency and further work is recommended to understand those parameters. Additional observations were made that suggested segmentation is not a mode of mixing. Segmentation modeled as an impedance pump can induce cyclical pressure heads that may contribute to flow in the intestine.

Thesis Supervisor: Anette Hosoi
Title: Associate Professor of Mechanical Engineering

Acknowledgements

I would like to thank my thesis advisor, Anette "Peko" Hosoi; she has been so positive and challenged me to be the driver behind my research. She put me in the guiding hands of my graduate student, Dawn Wendell, without whom, I would have never been able to conduct this research. Dawn led me calmly and taught me about the complexities of research. Her "don't worry" attitude and excitement for research fostered my own passions.

I would like to thank Dr. Barbara Hughey for helping me with all of my instrumentation trouble and for her constant encouragement to go to graduate school. Also, to Brian Ruddy, for lending me a power supply when I couldn't find a working one.

Finally, to my family, who have supported me unconditionally during my four years here at M.I.T. and in all of my ventures thus far.

Table of Contents

Chapter 1

Introduction

Some of the best engineering principals were invented by nature. Naturally occurring processes have had thousands and sometimes millions of years to evolve, change, and perfect themselves. Humans have been trying to understand and learn how to replicate nature throughout evolution.

The human body, though, remains one of nature's most mysterious specimens. Thousands of processes go on in the human body that scientists and engineers alike don't fully understand. While understanding of the human body is improving with time, engineers have begun to nature in order to better understand the function of biological processes.

1.1 The Small Intestine

One area of the human body that still lacks significant understanding is the small intestine. The small intestine is responsible for the transportation, digestion and absorption of the chyme, or digesta, that exits the stomach. There are three distinct motility patterns that drive digestion: peristalsis, pendular contractions and segmentation [4]. While all three motility patterns contribute to the digestion process in the intestine, the net fluid movement caused by each motility pattern is not very well understood [32]. Of all the motility patterns, segmentation is predominately misrepresented in the literature [4, 8, 29, 32].

1.1.1 Intestinal Segmentation

Segmentation is defined as the stationary contraction and relaxation of segments of the circular muscle layers encompassing the intestine. The contraction frequency decreases down the length of the intestine from about twelve to nine contractions per minute, or about 0.20 Hz at the oral end and about 0.15 Hz at the aboral end. [4].

Segmentation in the intestine has been described as a process that divides and recombines the intestinal content, but does not cause any net fluid propulsion [4, 8, 29]. This theory, though, was challenged by Macagno & Christenson who experimentally determined that two circular contractions could produce pumping and flow when the pumps were actuated with the same frequency, but with a phase lag [20].

In his editorial review to summarize a unified theory for fluid movement in the intestine, William Weems points out that "Recognitions limited to the fact that...segmentation mixes luminal fluid in a tube ignores a variety of other observations and questions that are extremely relevant to intestinal motility." He goes onto to suggest that an understanding of the intestine is only going to be achieved through systematically analyzing the system [32] as was begun by Thueneberg [29].

1.2 Impedance Pumping

Impedance is the resistance of a medium to transmit waves and is dependent on the frequency properties of the transmitted wave [1]. Whenever two mediums connect, part of the wave will be reflected where the percentage reflected is a function of the change in impedance.

Impedance pumping can therefore be defined as a type of valveless pumping where a pliant tube is connected to two rigid tubes of different impedance; as the pliant tube is compressed asymmetrically from the rigid ends, a net pressure is induced [9, 10, 11]. The pressure is caused

by the partial reflection of the waves from one end of the tube joining the reflected waves from the opposite side of the tube. As the waves interfere constructively and destructively, a net pressure head is induced on one side.

Extensive work has already been done to understand different aspect of an impedance pump. In 1954, Gerbert Liebau demonstrated valveless pumping by periodically compressing an elastic tube and showed that fluid could be pumped to higher pressure head [17, 18, 19]. He made attempts to understand which parameters were influencing his experimental set up—such as elasticity, viscosity, and inertia—but he was unable to understand what was actually contributing to the pumping.

Further work has gone on to expand the analytical [3, 15, 16, 23, 25, 26, 28, 33] and computational [5, 12, 13, 14] studies in an attempt to characterize impedance pumping, while experimental results are just beginning to have an impact [9, 10, 11, 17, 21, 23]. The most recent experimental study of impedance pumping was done by Hickerson, et al [9, 10, 11]. Hickerson aimed to understand the characteristic behaviors of the impedance pump and discover which characteristics dominate the response. While Hickerson advanced the understanding of the impedance pump, her results were primarily focused on a closed loop system and a net flow response. Her experimental study examined frequencies ranging 1-10Hz. Hickerson's experimental results suggested that a net flow was generated at each driving frequency and that as frequencies increased, certain resonant peaks began to occur. However, a complete understanding of the pressure responses that generated those flows remains elusive.

1.3 Motivation and Summary

The motivation for this thesis is to further understand the fluid dynamics of segmentation in the intestine by assuming that turns and twists in the intestine cause impedance changes, thus segmentation could be considered an impedance pumping problem.

This thesis assumes that segmentation in the intestine is caused by impedance changes of the organ as it twists, turns and folds back on itself. It aims to understand the response of an impedance pump on a physiologically realistic geometry at both physiological speeds, to understand pressure responses caused by segmentation. The system was validated at higher speeds as those tested by Hickerson, et al [9, 10, 11].

In the next chapter, we describe the experimental set up used to test the model of segmentation as an impedance pumping problem. In Chapter 3, we present and discuss the results of our experiment. Finally, in Chapter 4, our conclusions and future work are presented.

Chapter 2

Methods and Implementation

To understand the effects of impedance pumping at physiological and higher frequencies, an experimental set up was designed and manufactured to replicate the process of segmentation in the human intestine. The system was designed to operate at a range of frequencies, from below frequencies recorded during segmentation through higher frequencies as those tested by others [9, 10, 11]. As a result, impedance pumping and thus segmentation could be recorded to further understand the fluid dynamics of the intestine and to elaborate on Hickerson's [9, 10, 11] findings by applying them to an open loop system.

2.1 Apparatus

An experimental apparatus was built based upon the physiological characteristics of segmentation in the intestine (see Figure 2.4). It consists of three parts: an open loop system, a compression mechanism, and an actuation stage. The actuation stage gears down a motor to operate the compression mechanism which pinches a pliant tube in the open loop system. As the pliant tube is pinched, a known amount of fluid is displaced. Manometers at both ends of the open loop system record the height of the water as it changes due to wave interference and the known volume change.

By recording the change in height of the water at both ends of the open loop system, a pressure change, ΔP, can be found as a function of the height difference, Δh, between the manometers at both ends of the open loop system as:

$$\Delta P = \rho g \Delta h, \tag{2.1}$$

where ρ is the density of the fluid and g is the gravitational acceleration. In Equation 2.1, the change in pressure is only associated with the wave interactions induced by the compression mechanism. The volume change causes the same change in height on both ends of the open loop system. The constant volume change causing the same change in height on both sides was verified by positioning the pinchers in their fully closed position and measuring the change in height of the water in both manometers. It was the same. Therefore by taking the difference in the heights of the water at each time step, the change in height will be due to the wave interactions and pressure build up due to the impedance changes of the tube.

2.1.1 Open Loop System

The open loop system is comprised of several sections: the manometers, the pliant tube, the rigid connections, and valve mechanism. The manometers are hard-wall rigid clear PVC tubing with an inner diameter of 3/16" and a height of 11.5". The pliant tube is a poly-ethylene tube made by ULINE with a diameter of 0.700" and wall thickness of 0.004" [30]. The overall length of the plaint tube is 62.23 cm. The pliant tube is connected to the manometers using standard ½" PVC pipe with the appropriate fittings and an extra armed valve mechanism for filling. All of the sections are joined by Amazing Goop [7], an adhesive and sealant for plumbing projects. An illustration of the open loop system can be seen in Figure 2.1.
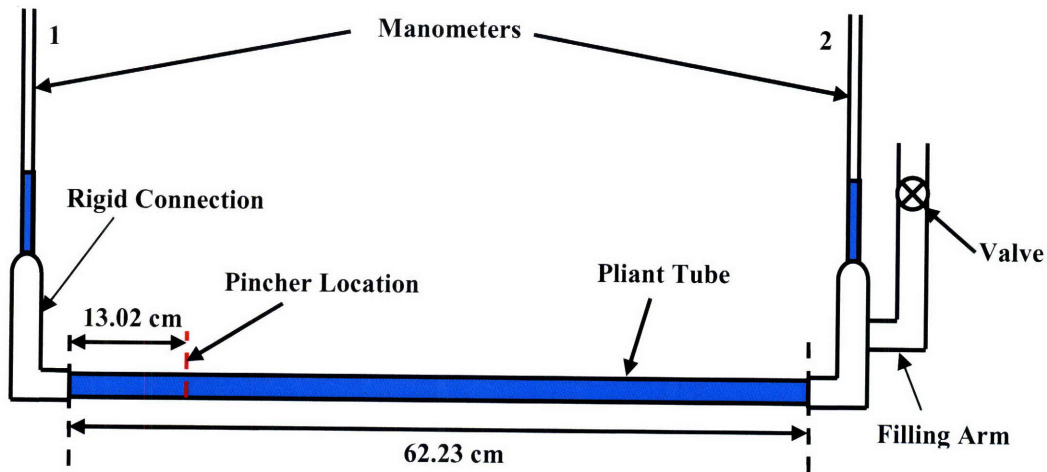
Figure 2.1 Open Loop System comprised of a pliant tube rigidly connected to two manometers at either end of the system. An extra arm of rigid PVC branches off manometer 2 and is used as a filling mechanism for the system. The compression mechanism compresses the pliant tube at the pincher location in the drawing.

For simplicity, the manometer and side that is closest to the pinching location will be called manometer 1 and side 1, while the manometer and side that is farthest from the pinching location will be called manometer 2 and side 2. For all experiments, the compression mechanism is positioned at the pincher location which is 13.02 cm from the rigid connection on side 1.

When filling the open loop system, a careful procedure is followed. First, the valve in the filling arm is opened and water is poured into the system until the valve is covered in water. At this point, water is visible within the manometer tubes. Then, the valve is closed, such that the entire filling arm is full of water and no air. Once the seal on the valve is secure, manometer 1 is slowly lowered, removing approximately 4 cm of water from the manometers. At this point, the height of the water in the manometers is lower than the height in the filling arm. The water in the filling arm cannot escape, though, because of the vacuum created by closing the valve. Once the system is filled and the height in the manometers adjusted in order to allow for the

appropriate volume change induced by the compression mechanism, the system is allowed to settle. The pliant section of the tube is massaged by hand until all bubbles release from the inside lining of the pliant section. Once the air bubbles are released, the open loop system was allowed to sit for more than 12 hours before any testing began.
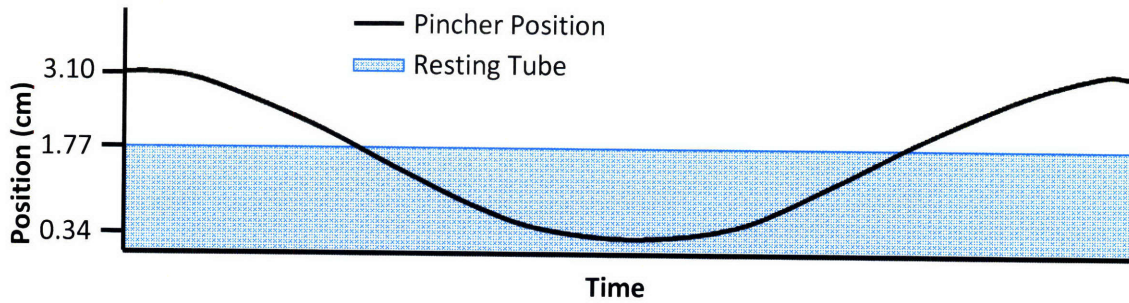
2.1.2 Compression Mechanism

While segmentation is a circumferential compression, our model aimed to simplify the process by only pinching the tube in one direction. The mechanism can be seen in Figure 2.2 below:
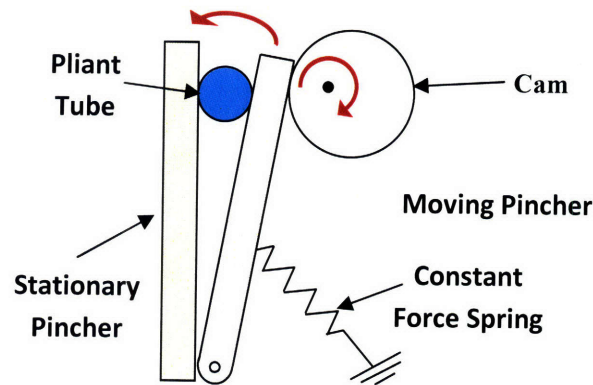
Figure 2.2   Compression Mechanism consists of two pinchers—one stationary and one moving. A constant force spring keeps the moving pincher pressed against a rotating cam. As the cam spins, the moving pincher compresses the pliant tube against the stationary pincer.

The compression mechanism acts like a pair of kitchen tongs—a compression force is applied and a spring restores the tongs to their original position; a rotating cam applies the compression force. As the cam is driven, it pushes the moving pincher toward the stationary pincher, compressing the pliant tube between the pinchers. The moving pincher maintains contact with the cam by a constant force spring.

The cam rotates creating a sinusoidal motion as seen in Figure 2.3. The tube is compressed to approximately 20% of its original diameter.

Figure 2.3 Compression Profile in Time. The compression mechanism creates a sinusoidal motion of the moving pincher toward the stationary pincher.

2.1.3 Actuation Stage

The actuation stage connects the actuating device to the compression mechanism. The two-stage low-frequency actuation set up is shown in Figure 2.4:
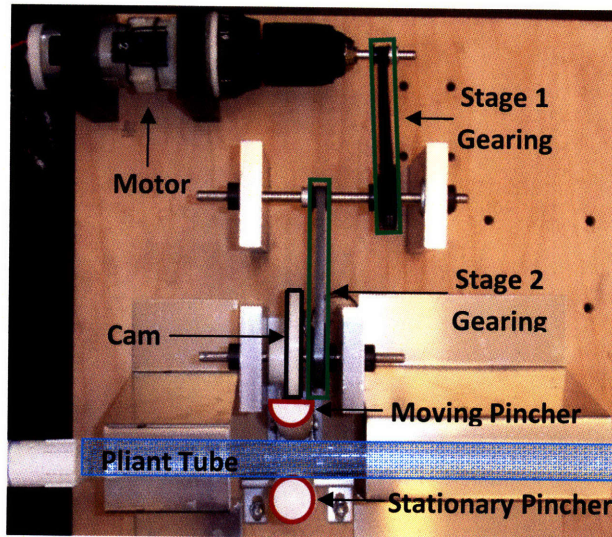
Figure 2.4 Low Frequency Actuation Stage uses two stages of gearing to enable actuation at physiological frequencies.

The motor is geared down twice to enable actuation at physiological frequencies. The actuation device is a 14.4V Milwaukee ½" Driver-Drill 0612-20 [22] disassembled and plugged into an HP E3632A power supply [2]. To enable examination of higher frequencies such as those

14

investigated by Hickerson, et al [9, 10, 11] the set up can be re-configured to enable a single stage actuation such that the motor directly drives the cam shaft. For both actuation set ups, the drill motor is kept in the high torque, low speed regime. The single stage actuation set up will be referred to as the high-frequency set up for simplicity. It is seen in Figure 2.5 below:
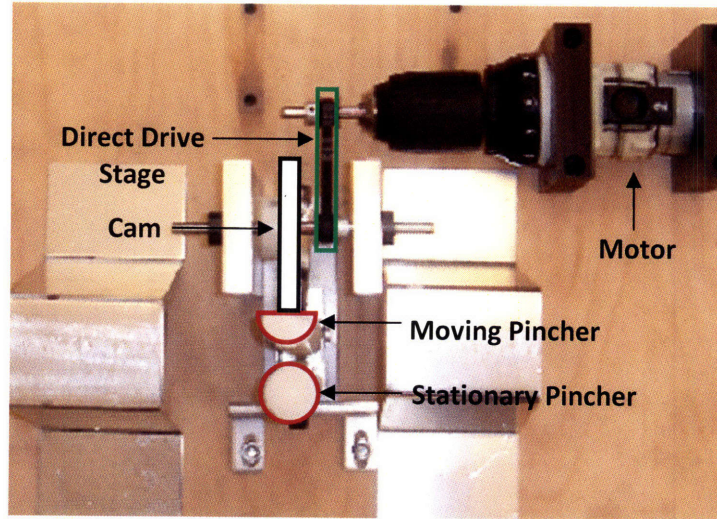
Figure 2.5 High Frequency Actuation Stage. The high frequency set up consists of a direct drive stage from the motor to the cam shaft.

2.2 System Calibration

For both actuation stage set ups, the systems need to be calibrated such that a compression frequency could be found given the voltage indicated on the power supply. Both the high-frequency and low-frequency actuation stage set ups were calibrated. For the low-frequency actuation set up, the system was set to a known voltage, as displayed on the power supply, then a Survivor II Accusplit XL stop watch was used to time a known number of cycles. One cycle is defined as the time it takes for the set screw in the cam to rotate 360°. The compression frequency, f_{comp}, was determined as:

$$f_{comp} = \frac{No.\, of\, Cycles}{Time} \tag{2.2}$$

For the high-frequency set up, the cam was rotating faster than could be reasonable timed using a stop watch. As a result, a Cole-Parmer 08199 Optical Tachometer was used [6]. A strip

15

of reflecting tape was secured to the edge of the cam. Once the compression mechanism was actuated, a reading was taken by placing the tachometer over the cam. The device recorded the speed of the cam in revolutions per minute (rpm) which were then converted to Hertz. Three readings were recorded at each voltage. Voltage was plotted to the average compression frequency and a linear fit agreed to within 3% as can be seen in Figure 2.6:
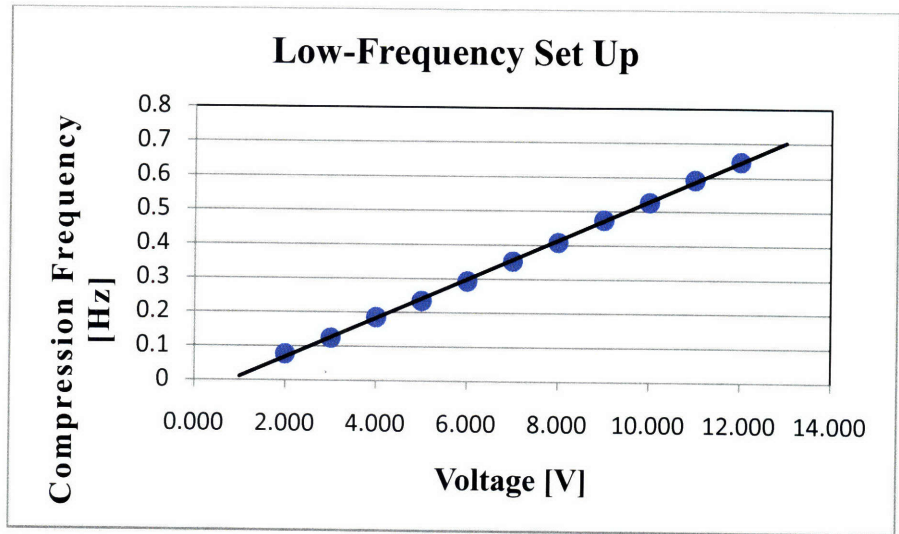
(a)
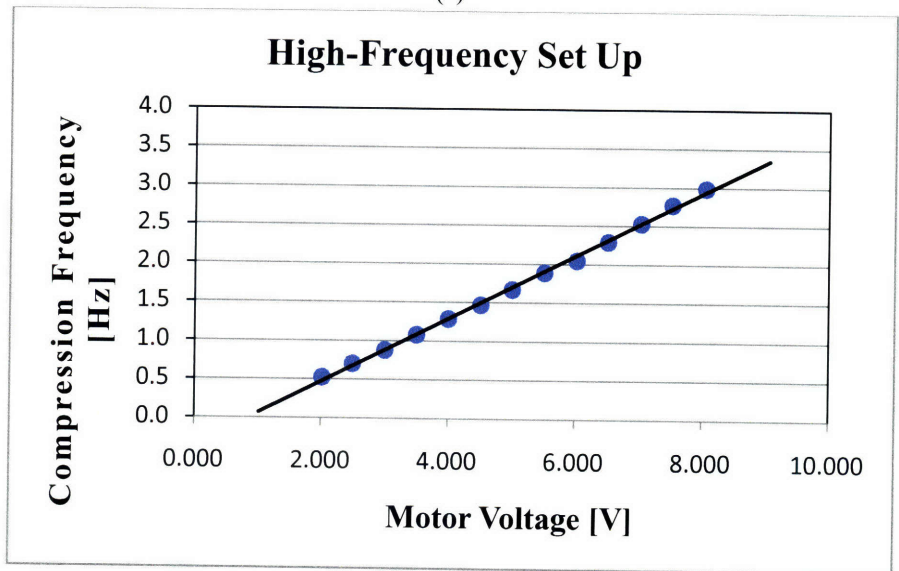
(b)

Figure 2.6 System Calibration of the power supply output voltage to the compression frequency of the compression actuation Part (a) is the low-frequency set up and part (b) is the high-frequency set up. Error bars on each point are less than 3%.

The voltage to compression frequency conversion equations are presented in Table 2.1 below. For the remainder of this study, results will be displayed as a function of compression frequencies rather than voltages.

Table 2.1 Calibration Equations to convert the output voltage from the power supply to the compression frequency of the compression mechanism.

Calibration Equation	
Low Frequency	$f_c = 0.058 \times \textit{Voltage} - 0.048$
High Frequency	$f_c = 0.407 \times \textit{Voltage} - 0.346$

2.3 Experimental Measurement

To complete the set up, a Sony Handycam HDR-SR5 [27] video camera is used to record the experiment in standard definition (SD) at a frame rate of 29 frames/second. It is positioned on a tripod at a distance such that the entire open loop system is in the frame of the camera. It is also raised so that the camera is approximately level with the settled water height in the manometers. The camera is also leveled such that the lens is parallel to the experimental set up.

In order to increase the visibility of the water, approximately 20 drops of green dye is added. A piece of 4.25" by 11.0" white paper is taped to the back side of each manometer to improve the contrast. The paper also serves as a reference for the image processing and analysis.

The experimental procedure begins by allowing the system to settle. The open loop system is secured in its stand and the fluid is allowed to come to rest. A permanent marker is used to mark the paper with the settled height of the water. The distance between the pinchers and side 1 of the open loop system is measured and re-positioned until it is at 13.02cm. The power supply is turned on and the output voltage recorded. The compression mechanism begins pinching the pliant tube. After 30 seconds, the video camera is turned on using a remote control and records approximately 30 seconds of pumping.

17

The voltage is then increased on the power supply. Once again the system is given 30 seconds to adjust to the new compression frequency. The camera is turned on again and records for approximately 30 seconds. This process is repeated from 0.126-0.59 Hz in approximately 0.058 Hz increments for the low-frequency and from 0.874-4.53 Hz in approximately 0.41 Hz increments for the high-frequency set up.

2.4 Image Processing

The raw video footage is transferred from the camera as a movie file (.mpg). First, it is converted by AVS Video Converter [24] to a Quicktime movie (.mov) with an H.264-best quality video format using the original frame rate of 29 frames/second and original frame size 720x400 pixels and an audio format of MP2/4(AAC LC) – 320kbps at a frequency of 48kHz.

The video was analyzed using LoggerPro 3.6.0 [31]. Each video was imported into its own worksheet. The "correct aspect ratio for DV movies" was unclicked under movie options in order to restore the original frame size.

Two analysis parameters were set for each video—the x-y origin of video and measurement reference. The origin was set near side 1 with the x axis running through the pre-marked settled water level on the white pieces of paper. Setting the origin here enables every reference height to be made from the settled level. The measurement reference was drawn using the height of white paper taped to the back of the manometers; it was recorded in the program as 11.0". LoggerPro automatically uses this measurement reference to assign a value to each pixel.

For each video, three data sets are defined. Data set x:y is the x and y positions of manometer 1. Data set x2:y2 is the x and y positions of manometer 2. Data set x3:y3 is the x and y positions and times for the pinchers. For the first two data sets, a mark was made at the height of the water in the manometer for each frame of the video for its entirety. For the third

18

data set, a mark was made each time the pinchers where in their fully compressed position. The third data set enables analysis based on compression cycles. For all data sets, the time is recorded at each frame.

The height of the water in each manometer as a function of time is used to find the difference in pressure between the manometers as a function of time using Equation 2.1 where g=9.81 m/s^2 and ρ=1000kg/m^3. As a standard, the change in height is recorded as:

$$\Delta h = h_2 - h_1 \qquad (2.2)$$

where h_2 is the height in manometer 2 and h_1 is the height in manometer 1. The change in pressure as a function of time is determined for each pressure cycle, which will be discussed further in the next chapter.

2.5 Reynolds Number

The Reynolds number is a ratio of inertial forces to viscous forces that show the relative importance of these two forces for given flow conditions. It is defined as:

$$Re = \frac{v_f L}{v} \qquad (2.3)$$

where v_f is the velocity of the fluid, L is a characteristic length, and v is the kinematic viscosity of the fluid. For the experimental apparatus described above, the Reynolds number inside the compliant tube is important to understand which of these forces is dominating the response. It can be found knowing the velocity of the fluid in the manometers and the geometric relationship between the manometers and the compliant tube. Thus, the velocity of the fluid in the compliant tube can be defined in terms of the height in the manometer, ΔH, over which the fluid oscillates, the frequency of compressions, ω, and the diameters of the compliant tube, D_c and the manometers, D_m:

$$v_f = \Delta H \omega \frac{D_m{}^2}{D_c{}^2} \tag{2.4}$$

Note that ΔH is the change in height of fluid in one manometer and therefore does not equal Δh.

Using the diameter of the compliant tube as the characteristic length for this apparatus, the

Reynolds number becomes:

$$Re = \frac{\Delta H \omega D_m{}^2}{v D_c} \tag{2.5}$$

Chapter 3

Results and Discussion

3.1 Pressure Response

For each tested frequency, a unique pressure response resulted. The response varies for each frequency tested due to the constructive and destructive wave interferences that result from the impedance change at either end of the pliant tube. An example of such a response is presented in Figure 3.1 below:
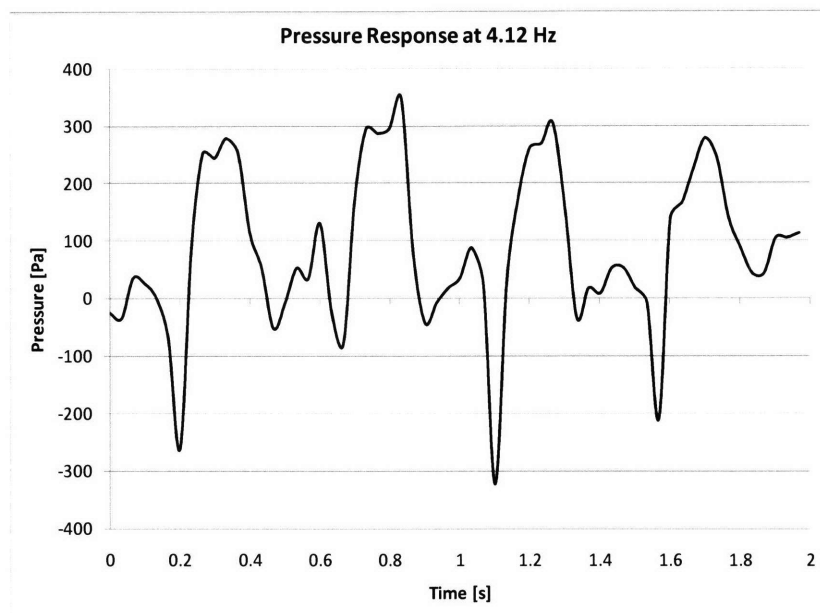
Figure 3.1 Pressure Response at 4.12 Hz shows an example of a systematic response at a single driving frequency.

Figure 3.1 above demonstrates the cyclical nature of the response that results from a single driving frequency. As the pliant tube is compressed, it generates waves in either direction. The wave reaches manometer 1 and partially reflects before it reaches manometer 2. As the two reflections meet, they interfere with each other, either constructively or destructively.

The cycle repeats and the waves cyclically cause a change in pressure between the two manometers. The change is most likely attributed to the wave speed in the given medium and the timing of the compressions. All of the results presented examine the system after a "steady state" has been reached and the system falls into a regular cyclical pattern.

The Reynolds Numbers range from 13-1350 which is a transitional range from viscous forces dominating the response to inertial forces. This transitional range suggests that both forces are comparably influencing the flow, and therefore, the pressure.

3.2 Low Frequency Response

For the low frequency set up and regime tested, an interesting response was observed that has not been previously documented for open loop systems. In Figure 3.2, two pressure responses are shown—a dimensionless pressure response and a measured pressure response—as a function of dimensionless time, $\underline{t}$, where $\underline{t}$ is defined as:

$$\underline{t} = \omega t \tag{3.1}$$

where ω is the compression frequency in Hertz and t is time in seconds.

The pressure response is affected by both the inertial and viscous forces comparably, therefore, there are two methods to make pressure dimensionless. For conventionality, dimensionless pressure, $\underline{P}$, will here forth be described as:

$$\underline{P} = \frac{P D_c}{\mu v} \tag{3.2}$$

22

where P is the measured pressure, D_c is the diameter of the compliant tube, μ is the viscosity, and υ is the velocity in the compliant tube.
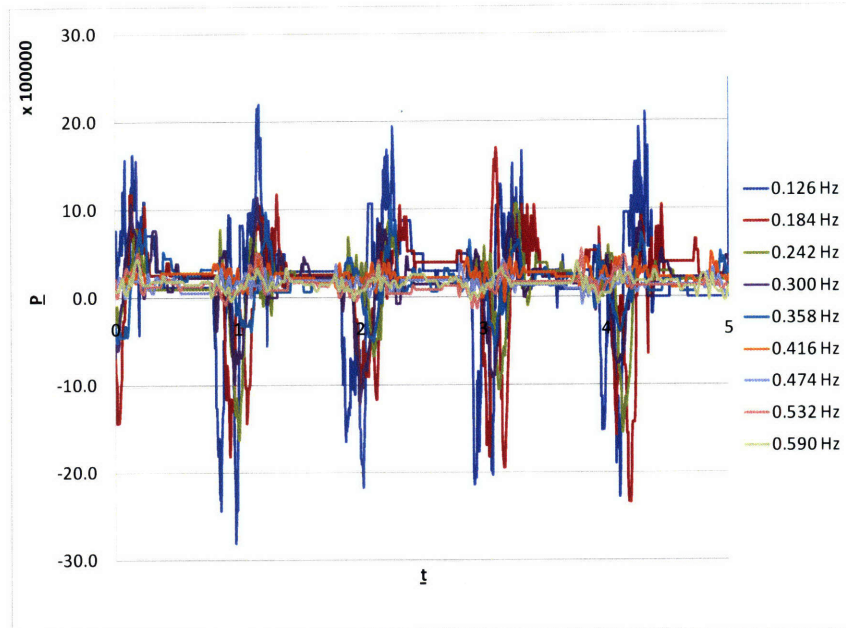
(a)
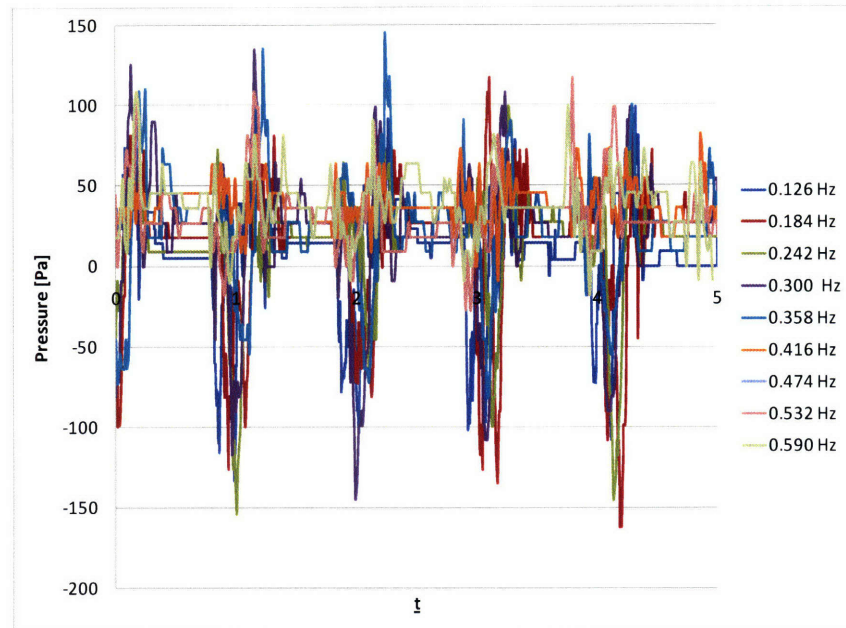
(b)

Figure 3.2 Pressure Response due to Compressions for Low Frequency Regime. Both (a) and (b) show different representations of pressure as a function of time. In (a), the dimensionless pressure is plotted, while the dimensional pressure is plotted in (b).

23

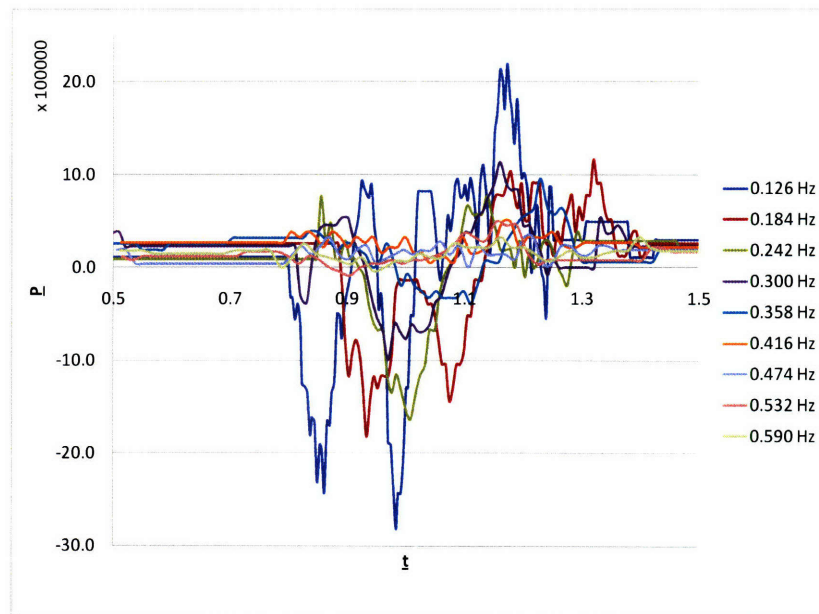In Figure 3.2 (a), the dimensionless pressure response shows decreasing magnitude with increasing frequency. The generally responses are amplified at lower frequencies and smaller at higher frequencies. As compared with Figure 3.2 (b) where the pressure responses are very similar for all the tested frequencies, the response is more complicated than can be understood from a dimensionless pressure viewpoint. A single compression cycle for all frequencies can be seen in Figure 3.3 below:

Figure 3.3 Single Dimensionless Pressure Response. Dimensionless pressure response for a single compression.

For the low frequency response shown in Figure 3.2 (b), the pressure spikes are highly cyclical with compressions, as expected. As the tube is compressed, manometer 1 fills before manometer 2. As a result, there is a large negative pressure change. As the tube begins uncompressing, the height of water in manometer 2 goes down after manometer 1 and there is a positive pressure change. The time delay that is seen from manometer 1 to manometer 2 is not due to the pressure wave taking longer to arrive at one manometer than the other because the delay captured by the camera is approximately 80 times slower than the expected delay due to

24

the pressure wave. The time delay is not fully understood and further work and analysis is needed to better understand the properties causing this delay.

For the low frequency response below 0.300 Hz, there tends to be more of a net negative pressure than a net positive one. There is a transition region, though, around 0.300 Hz where the net positive pressure and the net negative pressure are approximately equal. Above 0.358 Hz, the net positive pressure tends to be greater than the net negative pressure. This changing region suggests that flow will be stagnant in this regime. Above and below this regime, the flow will be moving in opposite directions. It is probable that this results from the impedance changes of the tube and the interfering pressure waves. The responses are all of similar magnitude, though, and fall between about -150 to 150 Pa.

The net pressure overall suggests that flow could be generated even at these low compression frequencies. In terms of the physiological phenomenon of segmentation, it is possible that segmentation contributes to flow of digesta down the intestine. While water does not exhibit the non-newtonian characterists of the viscous shear-thinning digesta, it does suggest that a net pressure head can be created in an open loop system under impedance pumping which exhibits similar characteristics as the pumping attributed to segmentation.

The steady state result is cyclical. One compression results in a full response of the system, enabling it to come to rest between each compression. The system does not see a resting pressure of zero in all cases. It is possible that this is due to the camera not being exactly lined up correctly or due to air bubbles getting trapped in the system as the water heights oscillate.

3.3 High Frequency Response

The high frequency response can be seen in Figure 3.4. As the frequency is increased the waves begin to interact with each other and do not have time to come to rest between compressions.

Each compression contributes a wave that will constructively or destructively interfere with those already moving in the system.
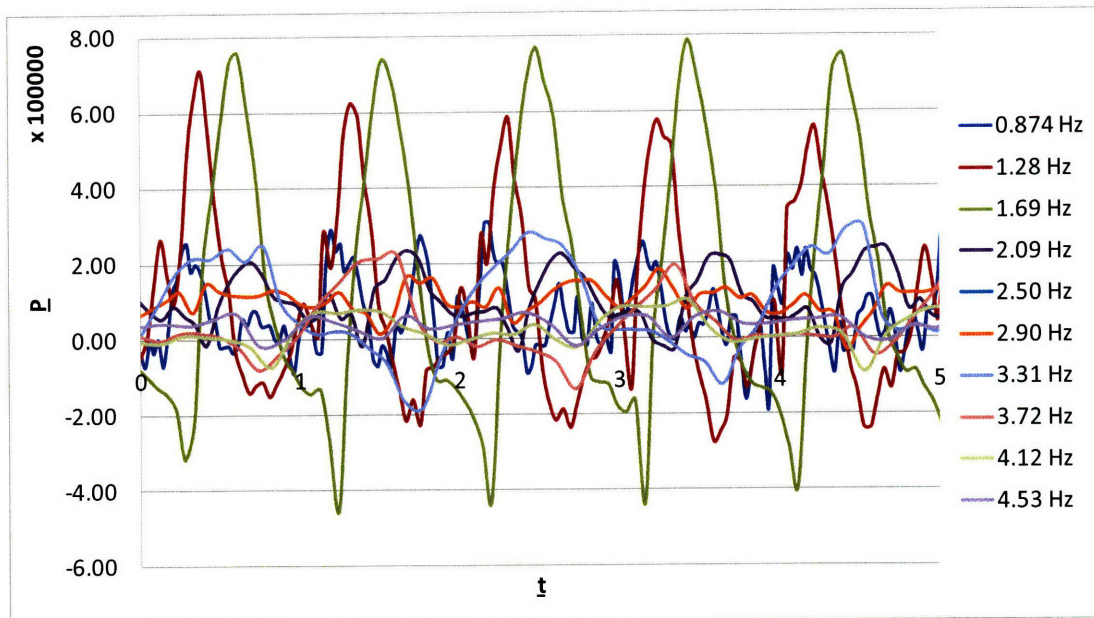
(a)
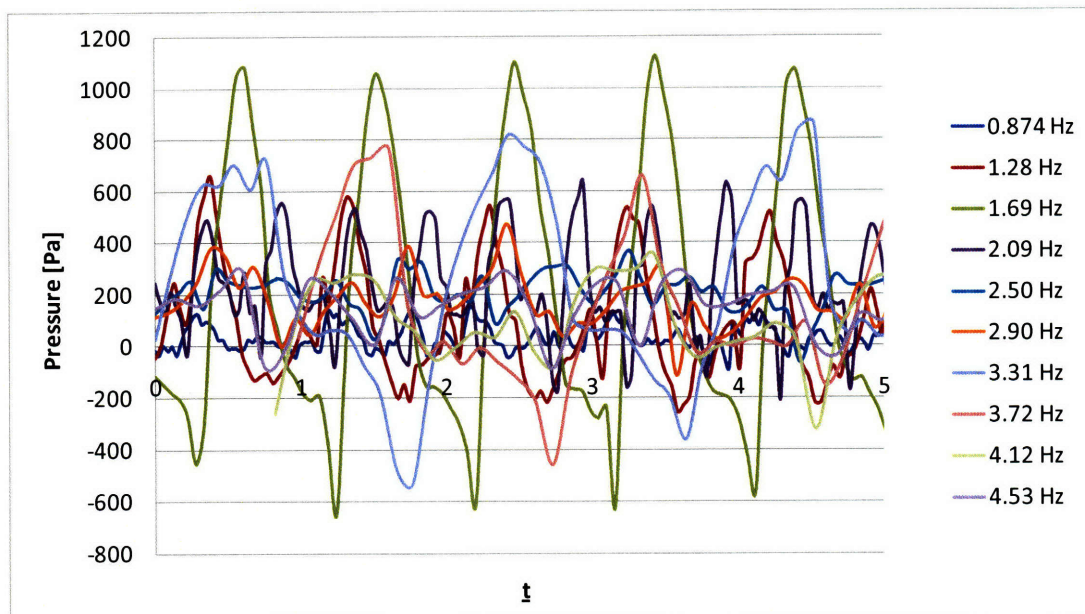
(b)

Figure 3.4 Pressure Response due to Compressions for High Frequency Regime. Both (a) and (b) show different representations of pressure as a function of time. In (a), the dimensionless pressure is plotted, while the dimensional pressure is plotted in (b).

As a result, there is an increase in the overall magnitude of the pressure responses that are seen. The compressions add momentum to the consecutive wave until an equilibrium is reached. As the compression frequency increases, the magnitude of the pressure responses also tends to increase. The dimensionless frequency response, once again, demonstrates the complexity of the systems response and further analysis is needed to fully understand the driving forces behind the systems response.

In Figure 3.4 (b), several differences exist from the responses seen in the low frequency response. The general band of pressure responses falls between -200 to 400 Pa, which is higher than those exhibited at lower compression frequencies. Additionally, the positive pressure peaks are higher than the negative pressure peaks. There was no transition regime, as seen at low frequency or net pressure change. This suggests that fluids compressed within these frequencies would flow in the same direction. It is quite obvious from the videos that at these higher frequencies manometer 2 rises while manometer 1 falls, causing a positive net pressure change. As the system progresses through its cycle, manometer 1 rises while manometer 2 falls, but the absolute change is not as great, therefore the net negative pressure is smaller in magnitude than the net positive pressure.

In Figure 3.4(a), the high frequency response shows a similar decreasing magnitude with increasing frequency as seen in the dimensionless low pressure response. An anomaly exists, though, at 1.69 Hz. In both the dimensionless and measured pressure responses, 1.69 Hz exhibits the largest "peak pressures". This phenomenon is most likely due to the natural frequency response of the system. The pressure response increases with increasing frequency toward a natural frequency of the system. The natural frequency is the point at which compressions are causing complete constructive interference and the pressure is at its highest. Increasing or

decreasing the compression frequency near that natural frequency will cause a decrease in the maximum pressure. Figure 3.4(b) shows that a natural frequency is neared at a compression frequency of 1.69 Hz as discussed earlier. At this frequency, each compression causes a pressure spike that is higher than all the rest.
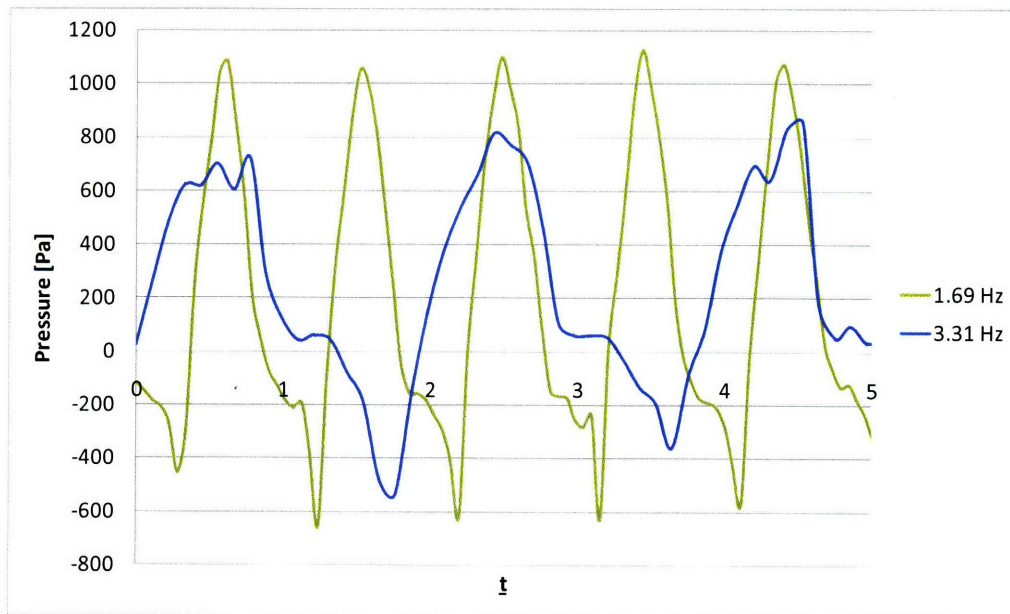
Figure 3.5 Frequency Doubling. The pressure is documented versus dimensionless time as a frequency near the natural frequency is doubled and observed.

If 1.69 Hz is indeed near the natural frequency of the system, then frequency doubling should cause another pressure spike. For the compression frequencies tested in this experimental set up, a frequency doubling is seen near 3.31 Hz. The natural frequency and its doubled frequency can be seen in Figure 3.5. The frequency near the natural frequency shows a pressure spike at each compression. The doubled frequency shows a spike every other compression. It spikes negatively on the off compressions. This frequency doubling response takes twice the dimensionless time to execute, but in real time, the responses are equally timed. By making time dimensionless, the response at 3.31Hz looks as though it's going half as slow, but in real-time, the pressure response are in phase.

The doubled frequency pressure response is smaller in magnitude than the natural frequency pressure response. This suggests that the natural frequency is actually slightly higher or slightly lower than compression frequencies explicitly stated. It can be inferred from figure 3.4 (b) that the actual natural frequency is slightly higher because as you increase and decrease the frequency near the doubled natural frequency, the magnitude of the pressure response at 3.72 Hz is significantly higher than at 2.90 Hz.

While it seems viable to find the net pressure per cycle, defining a "cycle" was quite challenging. Several different approaches were attempted. For example, a pressure cycle was defined as the time it takes for the pressure response to make a full loop, but the pressure cycles were not always consistent from cycle to cycle due to the complexity of the response. A cycle was also defined in terms of compressions, but due to the compression doubling that occurred after frequency doubling, it failed in terms of consistently defining a cycle for all the responses. As a result, trying to define a "net pressure" generated at each frequency was almost impossible because trying to define the cycle over which that pressure acted failed to accurately display the complexity of the system's response.

3.4 Mixing Observations

When the apparatus was first being set up, the open loop system contained un-dyed water. In order to observe the mixing phenomenon, the camera was turned on to record how the dye spread through the system when it was added through one of the manometers. When the dye was added to the water, the system was set to run in the high frequency set up. Initially, it was set to a compression frequency of 1.28 Hz. As soon as the dye hit the top surface of the water in the manometers, it diffused into the water in the manometers. The dye did not however mix in with the rest of the water (see Figure 3.5). The compression frequency was increased through the full

range under which the system operates and at no point did actuating the system cause the dye to mix with the system.
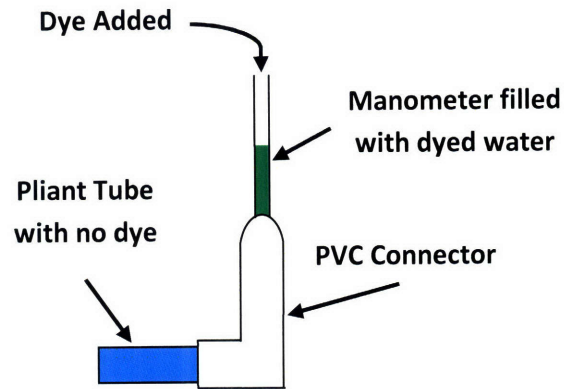
Figure 3.5 Mixing Observations. The dye is dropped into the top of the manometer while the compression mechanism is running. The dye quickly mixes with the oscillating water in the manometer tube, but that mixing does not cause the dye to mix with all of the water in the system. As seen above, the dye does not move around the corner of the PVC connector and mix with the fluid in the pliant tube even though the system is completely open.

When no mixing was observed, the system was shut off and the dye allowed to move through the fluid via diffusion.

While this observation is not directly related to impedance pumping, it does however suggest that impedance pumping does not directly attribute to mixing. It suggests that the commonly accepted notion that segmentation causes mixing in the intestine may not be accurate.

Chapter 4

Conclusions and Future Work

4.1 Concluding Remarks

In summary, this thesis presents an experimental investigation of impedance pumping at both physiological frequencies, as those seen in the intestine due to segmentation, and at higher frequencies. It has demonstrated that in an open loop system, complex pressure responses result from constructive and destructive interferences of waves actuated by a compression mechanism. The pressure responses can cause net pressure heads at all compression frequencies. The net pressure heads were both positive and negative suggesting that the net flow caused by these pressure heads would induce flow in opposite directions depending on the frequency of compressions. The dimensionless pressure responses demonstrated the complexity of the response and showed that pressure response is not solely a function of the compression frequency. It was observed, though, that with increasing compression frequency the magnitude of the dimensionless pressure response decreased. Additionally, the system exhibits natural frequencies and frequency doublings that, when excited, cause pressure peaks approximately four times greater than the general response.

Finally, some general observations suggest that impedance pumping does not contribute to mixing and that the common notion that segmentation causes mixing in the intestine may not accurately describe the entire role of segmentation in the intestine.

4.2 Future Work

While this thesis just begins to understand impedance pumping in open loop systems, there are many unresolved issues. First and foremost, the dimensionless pressure response demonstrated the complexity of the systems characteristics. There are many factors that influence the response of the system. More analysis and experimentation will be helpful in understanding those unresolved issues and aid in providing a model of the system response.

Secondly, investigating the mixing properties of segmentation and impedance pumping experimentally will give engineers and scientists a better understanding of why segmentation occurs in the intestine. An interesting investigation would be to further define the property of mixing and possibly how mixing and flow work together.

Finally, the experimental apparatus can be improved using digital pressure sensors that will enable a finer and more accurate reading of the system. Additionally, an understanding of how flow is influenced by pumping in an open system will enable a direct understanding of how these pressure profiles influence the flow. Beyond that many parameters can be varied within the current set up:

- The distance between manometer 1 and the compression mechanism
- The geometry of the pliant tube
- The fluid can be varied to simulate multiple fluids such as:
  - Oil
  - Digesta

32

- Sludge

- Particle-fluid mixtures (slurries)

- The number of compression mechanisms and the distances between them

- The size of the entire mechanism

While these are just a few examples of what can be changed in order to better understand the limitations and opportunities of impedance pumping, there are many possibilities. Future work could aim to better understand impedance pumping in terms of the intestine or it could examine the potential for further applications as in ink jet printers, oil pumping, pressure or flow control, etc.

Bibliography

[1]   "Acoustic Impedance." *Encyclopedia Britannica.* 2008. Encyclopedia Britannica
        Online. 08 May 2008 <http://www.britannica.com/eb/article-9003572>.

[2]   Agilent Technologies. Santa Clara, California, USA. http://www.agilent.com.

[3]   Auerback, D., Moehring, W., and Moser, M., "An analytical approach to the Liebau
        problem of valveless pumping," *Cardiovascular Engineering: An International
        Journal,* vol. 4, no. 2, pp. 201-207, 2004.

[4]   Bray, J. J., Cragg, P. A., MacKnight, A. D. C., and Mills, R. G., "Digestive System"
        Lecture Note on Human Physiology, Malden, MA: Blackwell Sciene, Inc., pp. 480-
        481, 1999.

[5]   Borzi, A. and Propst, G., "Numerical nvestigation of the Liebau phenomenon,"
        Zeitschrift für angewandte Mathmatik und Physik, vol. 54, no. 6, pp.1050-1072, 2003.

[6]   Cole-Parmer Instrument Co. Vernon Hills, IL, USA. http://www.coleparmer.com.

[7]   Eclectic Products, Inc. Arrowsmith, Eugene, OR, USA.
        http://www.eclecticproducts.com.

[8]   Ehrlein, J., Schemann, M., and Siegle, M., "Motor patterns of small intestine
        determined by closely spaced extraluminal transducers and videofluoroscopy,"
        American Journal of Physiology—Gastronintestinal and Liver Physiology, vol. 253,
        no. 3, pp. 259-G267, 1987.

[9]   Hickerson, A.I., *An Experimental Analysis of the Characteristic Behaviors of an
        Impedance Pump.* PhD thesis, California Institute of Technology, 2005.

[10] Hickerson, A.I., and Gharib, M., "On the resonance of a pliant tube as a mechanism for valveless pumping," *Journal of Fluid Mechanics,* vol. 555, pp.141-148, 2006.

[11] Hickerson, A.I., Rinderknecht, D., and Gharib, M., "Experimental study of the behavior of a valveless impedance pump," *Experiments in Fluids,* vol. 28, pp. 534-540, 2005.

[12] Jung, E., *Two-Dimensional Simulations of Valveless Pumping Using the Immersed Boundary Method.* PhD thesis, New York University, 1999.

[13] Jung, E., and Peskin, C., "2-D simulations of valveless pumping using immersed boundary method," *SIAM Journal on Scientific Computing*, vol. 23, no. 1, pp. 19-45, 2001.

[14] Jung, E., and Peskin, C., "2-D simulations of valveless pumping using immersed boundary methods (ii)," 2001.

[15] Kenner, T., Moser, M., Tanev, I., and Ono, K., "The Liebau-effect on the optimal use of energy for the circulation of blood," *Scripta Medica,* vol. 73, no. 1, pp. 9-14, 2000.

[16] Kenner, T., "Biological asymmetry and cardiovascular blood transport," *Cardiovascular Engineer: An International Journal*, vol. 4, no. 2, pp. 209-217, 2004.

[17] Liebau, G., "Über ein ventilloses Pumpprinzip," *Naturwissenschaften*, vol. 41, pp. 327, 1954.

[18] Liebau, G., "Die Stromungsprinzipien des Herzens," *Zeitschrift für Kreislaufforschung*, pp.677-684, 1955.

[19] Liebau, G., "Die Bedeutung der Tragheitskrafte dur die Dynamic des Blutkrislaufs," *Zeitschrift für Kreislaufforschung*, pp. 428-438, 1956.

[20] Macagno, E. O., and Christensen, J., "Fluid Mechanics of the Duodenum," *Annual Review of Fluid Mechanics,* vol. 12, pp.139-158, 1980.

[21] Mahrenholtz, V. O., "A contribution to the pumping principal of periodically acting valveless pumps," *Forsch. Auf Dem Gebiet des Ingieurwesens,* vol. 29, pp.47-56, 73-81, 1963.

[22] Milwaukee Electric Tool. Brookfield, WI, USA. http://www.milwaukeetool.com.

[23] Moser, M., Huang, J. W., Schwarz, G. S., Kenner, T., and Noordergraff, A., "Impedance defined flow: Generalization of William Harvey's concept of the circulation – 370 years later," International *Journal of Cardiovascular Medicine and Science,* vol. 1, no. 3/4, pp. 205-211, 1998.

[24] Online Media Technologies, Ltd. London, United Kingdom. http://www.avs4you.com.

[25] Ottensen, J., "Valveless pumping in a fluid-filled closed elastic tube-system: one-dimensional theory with experimental validation," *Journal of Mathematical Biology,* vol. 46, no. 4, pp. 309-332, 2003.

[26] Rath, H. and Teipil, I. "Der Fordereffekt in ventillosen, elastichen Leitungen," *Zeitschrift für angewandte Mathmatik und Physik,* vol. 29, pp. 123-122, 1978.

[27] Sony USA. New York, New York, USA. http://www.sony.com.

[28] Thomann, H., "A simple pumping mechanism in a valveless tube," *Zeitschrift für angewandte Mathematik und Physik,* vol. 29, pp. 169-177, 1978. Swiss Federal Institute of Technology, Zurich.

[29] Thueneberg, L., and Peters, S., "Toward a Concept of Stretch-Coupling in Smooth Muscle. I. Anatomy of Intestinal Segmentation and Sleeve Contraction" *The Anatomical Record,* vol. 262, pp.110-124, 2001.

[30] ULINE Shipping Supplies. Chicago, IL, USA. http://www.uline.com.

[31] Vernier Software & Technology. Beaverton, OR, USA. http://www.vernier.com.

[32] Weems, W., "Intestinal wall motion, propulsion, and fluid movement: trends toward a unified theory," *American Journal of Physiology—Gastrointestinal and Liver Physiology,* vol. 243, no. 6, pp. G177-G188, 1982.

[33] Zhang, Y., Reese, J., Gorman, D., and Madhok, R., "The vibration of an artery-like tube conveying pulsatile fluid flow," *Proceeding of the Institution of Mechanical Engineers Part H—Journal of Engineering in Medicine,* vol. 216, no. H1, pp. 1-11, 2002.